

Characterizing planetary orbits and trajectories of light in the Reissner-Nordström metric

F.T. Hioe*

Department of Physics, St. John Fisher College, Rochester, NY 14618

March 7, 2014

Abstract

Exact analytic expressions for planetary orbits and light trajectories in the Reissner-Nordström geometry are presented. They are characterized in a map specified by three dimensionless parameters for the planetary orbits, while two dimensionless parameters are required to map the trajectories of light. Notable differences with the corresponding orbits and trajectories in the Schwarzschild geometry are indicated. In particular, when the energy and angular momentum of the planet are fixed, the precession angle of the orbit decreases as the net electric charge of the massive star or black hole increases. A similar result also holds for the deflection angle of a light ray.

PACS numbers: 04.20.Jb, 02.90.+p

1 Introduction

It is well known that besides the Schwarzschild spherically symmetric solution of Einstein's equation for the vacuum, there is the Reissner-Nordström (R-N) spherically symmetric solution of the coupled equations of Einstein and Maxwell [See e.g.1,2]. The R-N geometry applies to a massive object or a black hole with mass M and electric charge Q . Since we have not observed any large macroscopic body in the universe that possesses a net charge, the consideration of a charged massive object or black hole would appear to be unrealistic. Nevertheless, the study of the R-N solution is useful to our understanding of the nature of space and time. At the very least, one would like to know what the most notable effect of the presence of a net electric charge on a massive object is on the trajectory of an electrically neutral planet (which we shall call a particle) or a light ray outside the massive object. We shall refer to the massive object as a black hole even though most of the results that we present in this paper apply equally if it is simply a massive star. With the assumption that the charged black hole is centered at the origin of the coordinates, we shall present analytic expressions for all trajectories of particles and light in the polar coordinates (r, ϕ) in the equatorial plane $\theta = \pi/2$. Because the time coordinate has been eliminated

and is not present in our expressions, we do not discuss in this paper the many delicate questions about time when the particles or photons may cross the event horizon. We concentrate on the method that we have taken [3, 4] of putting all possible trajectories onto a universal map characterized by three dimensionless parameters and divided into regions with clearly defined analytic boundaries. On any given point of this map, the corresponding trajectory can be expressed in a simple analytic expression in terms of the Jacobian elliptic functions [5] with a predictable behavior. We shall also highlight the principal differences the electric charge on the black hole makes on the trajectories and how our analytic expressions reveal these differences.

Analytic expressions have been used before to describe the geodesics in Schwarzschild and in Reissner-Nordström metrics, mainly in terms of Weierstrass elliptic functions [5]. The Schwarzschild metric was treated using these functions in the early work of Hagihara [6] and Whittaker [7] while the R-N metric was analyzed in more recent papers for particles [8-11] and for light rays [12, 13] [see also other references therein]. As will become clear from the remainder of this Introduction and this paper, the ways these authors analyzed their analytic expressions and classified their trajectories are quite different from the method given in this paper and in our earlier papers [3, 4]. Our approach and treatment may be thought of as giving an alternative and useful perspective, in addition to some specific results that were not given previously. We should also mention that one of the earliest (but very brief) analytic works that made use of the Jacobian elliptic functions for the Schwarzschild metric is that of Forsyth [14].

We now discuss in more detail the approach that we use in this paper. Instead of the common practice of using the total energy, angular momentum, and generalized geometric eccentricity (which Chandrasekhar called E , L and e respectively in ref.2) for characterizing different trajectories in the Schwarzschild geometry, it was suggested in refs.3 and 4 that it is more convenient to put all possible trajectories of particles on a map specified by two dimensionless parameters. We follow the same procedure here but add an additional dimensionless parameter for the electric charge for the R-N geometry. We do not use units for which the universal gravitation constant G and the speed of light c are set equal to one, and, as in our previous work, we ignore the effect of gravitational radiation.

For particles in the Schwarzschild geometry, the two dimensionless parameters that we choose to represent the coordinates of the map are e^2 and s^2 which we called the energy and field parameters respectively that are defined by

$$e^2 \equiv 1 + \frac{h^2 c^2 (\kappa^2 - 1)}{(GM)^2} = 1 + \frac{\kappa^2 - 1}{s^2}, \quad (1)$$

and

$$s^2 \equiv \left(\frac{GM}{hc} \right)^2, \quad (2)$$

where κ is the total energy per unit rest energy of the particle, and h is the angular momentum per unit rest mass of the particle. The coordinates of this universal map for all possible particle trajectories are $-\infty < e^2 < +\infty$ and $0 \leq s^2 \leq +\infty$ [15]. One may of course use the coordinates (κ, s) with $0 \leq \kappa \leq +\infty$ and $0 \leq s \leq +\infty$ for the map [see ref.4 for some description of this]. Unlike κ and s that represent two independent physical quantities, namely, energy and angular momentum, e^2 is a (special) combination of these two quantities. The advantage of using (e^2, s^2) is that e^2 not only is a convenient combination of the total energy and angular momentum of the particle for all possible trajectories, but also that for small values of s^2 , e represents the true geometrical eccentricity of the Newtonian orbits for the entire range of $+\infty \geq e \geq 0$, and it alone, without s , can be used to characterize the Newtonian orbit of the particle. We should emphasize that in general our parameter e is not the same as the generalized geometrical eccentricity used by Darwin [16], Chandrasekhar [2] and many researchers (also denoted by e but its definition is different and its value can be complex the way they defined it). In the Newtonian limit, $c^2(\kappa^2 - 1)$ in eq.(1) becomes $2E_0/m_0$, where E_0 is the sum of the kinetic and potential energies of the particle, m_0 is the rest mass of the particle, and e becomes

$$e \simeq \sqrt{1 + \frac{2E_0 h^2}{m_0 (GM)^2}} \quad (3)$$

and is the geometrical eccentricity of the particle orbit. We should also emphasize that we generally use e^2 instead of e because e^2 can be negative. Indeed the negative values of e^2 are indicative of a non-classical general relativistic region that allows elliptic orbits with a non-Newtonian eccentricity [17]. The radial distance r of the particle from the black hole is expressed as

$$q = \frac{r}{\alpha}, \quad (4)$$

in units of the Schwarzschild radius α defined by

$$\alpha \equiv \frac{2GM}{c^2}. \quad (5)$$

The parameter space (e^2, s^2) is divided into two regions which we called Regions I and II [3,4]. Region I has bound, unbound, and terminating orbits, and Region II has terminating orbits only.

For particles in the R-N geometry, we need a third dimensionless parameter to measure the charge on the black hole. Noting that $GQ^2/(4\pi\epsilon_0 c^4)$, where ϵ_0 is the permittivity of free space, has the dimension of $(length)^2$, we define the dimensionless parameter

$$\beta^2 \equiv \frac{GQ^2}{4\pi\epsilon_0 c^4 \alpha^2}, \quad (6)$$

to be a measure of the electric charge on the black hole. Instead of using a parameter space with three coordinates (e^2, s^2, β^2) that are difficult to view,

we continue to use a parameter space with two coordinates (e^2, s^2) for a given value of β^2 , and show that the parameter space can again be divided into two regions but the boundary depends on the value of β^2 . We will see that it suffices for us to show the boundary separating the two regions for only two extreme cases for $\beta^2 = 0$ and $\beta^2 = 1/4$ from which one can see where the approximate boundaries are for the intermediate values of β^2 .

For the trajectories of light in the Schwarzschild geometry, it was shown in refs.3 and 18, following the suggestion of Martin [19], that they can be characterized by a single dimensionless parameter (denoted by U_1) which is related to the ratio κ/h of the energy and angular momentum of light. For the R-N geometry, we use the parameter space (U_1, β^2) and obtain the specific boundaries that divide the space into three regions.

2 Particle Trajectories in the R-N Geometry

We consider the Reissner-Nordström (R-N) geometry, i.e. the static spherically symmetric gravitational field in the space surrounding a massive spherical object such as a star or a black hole of mass M carrying a net electric charge Q . The R-N metric for the spacetime outside the black hole in the spherical coordinates r, θ, ϕ is [1,2]

$$dt^2 = c^2 \left(1 - \frac{\alpha}{r} + \frac{Q_*^2}{r^2} \right) dt^2 - \left(1 - \frac{\alpha}{r} + \frac{Q_*^2}{r^2} \right)^{-1} dr^2 - r^2 d\theta^2 - r^2 \sin^2 \theta d\phi^2 \quad (7)$$

where α is the Schwarzschild radius defined in eq.(5), and

$$Q_*^2 = \frac{GQ^2}{4\pi\epsilon_0 c^4}. \quad (8)$$

If $[x^\mu] = (t, r, \theta, \phi)$, then the worldline $x^\mu(\tau)$, where τ is the proper time along the path, of a particle moving in the equatorial plane $\theta = \pi/2$ satisfies the equations [1,2]

$$\left(1 - \frac{\alpha}{r} + \frac{Q_*^2}{r^2} \right) \dot{t} = \kappa, \quad (9)$$

$$c^2 \left(1 - \frac{\alpha}{r} + \frac{Q_*^2}{r^2} \right) \dot{t}^2 - \left(1 - \frac{\alpha}{r} + \frac{Q_*^2}{r^2} \right)^{-1} \dot{r}^2 - r^2 \dot{\phi}^2 = c^2, \quad (10)$$

$$r^2 \dot{\phi} = h, \quad (11)$$

where the derivative $\dot{}$ represents $d/d\tau$. The coordinates r and ϕ describe the position of the particle relative to the charged star or black hole centered at the origin. The constant h is identified as the angular momentum per unit rest mass of the particle, and the constant κ is identified to be the total energy per unit rest energy of the particle

$$\kappa = \frac{E}{m_0 c^2}, \quad (12)$$

where E is the total energy of the particle in its orbit and m_0 is the rest mass of the particle at $r = \infty$. Substituting eqs.(9) and (11) into (10) gives the 'combined' energy equation

$$\dot{r}^2 + c^2 + \frac{h^2}{r^2} \left(1 - \frac{\alpha}{r} + \frac{Q_*^2}{r^2} \right) - \frac{c^2 \alpha}{r} = c^2 \kappa^2. \quad (13)$$

Substituting $dr/d\tau = (dr/d\phi)(d\phi/d\tau) = (h/r^2)(dr/d\phi)$ into the combined energy equation gives the differential equation for the trajectory of the particle

$$\left(\frac{du}{d\phi} \right)^2 = -Q_*^2 u^4 + \alpha u^3 - u^2 \left(1 + \frac{c^2}{h^2} Q_*^2 \right) + \left(\frac{2GM}{h^2} \right) u + \frac{c^2(\kappa^2 - 1)}{h^2}, \quad (14)$$

where $u = 1/r$. We define the dimensionless inverse distance U from the following relation

$$\frac{1}{q} \equiv \frac{\alpha}{r} = \alpha u \equiv \frac{1}{3} + 4U. \quad (15)$$

In terms of U , eq.(14) becomes

$$\left(\frac{dU}{d\phi} \right)^2 = a_0 U^4 + 4a_1 U^3 + 6a_2 U^2 + 4a_3 U + a_4, \quad (16)$$

where

$$a_0 = -2^4 \beta^2, \quad (17)$$

$$a_1 = 1 - \frac{4}{3} \beta^2, \quad (18)$$

$$a_2 = -\frac{1}{9} \beta^2 (1 + 6s^2), \quad (19)$$

$$a_3 = -\frac{1}{4} \left[g_2 + \frac{1}{3^3} \beta^2 (1 + 18s^2) \right], \quad (20)$$

$$a_4 = - \left[g_3 + \frac{1}{2^4 \cdot 3^4} \beta^2 (1 + 36s^2) \right], \quad (21)$$

where β^2 is given by eq.(6) and where

$$\begin{aligned} g_2 &= \frac{1}{12} - s^2 \\ g_3 &= \frac{1}{216} + \frac{1}{6} s^2 - \frac{1}{4} \kappa^2 s^2 \equiv \frac{1}{216} - \frac{1}{12} s^2 + \frac{1}{4} (1 - e^2) s^4, \end{aligned} \quad (22)$$

s^2 , κ^2 and e^2 having been defined earlier in eqs.(2), (12) and (1). The dimensionless inverse radial distance U in place of α/r has been chosen so that, in the Schwarzschild limit $\beta^2 = 0$, eq.(16) reduces to the corresponding equation studied in refs.3 and 4 given by

$$\left(\frac{dU}{d\phi}\right)^2 = 4U^3 - g_2U - g_3. \quad (23)$$

Before we divide the parameter space (e^2, s^2) for a given β^2 into regions and present various analytic solutions of eq.(16) for the trajectories of the particle, we note from the factor

$$D \equiv 1 - \frac{\alpha}{r} + \frac{Q_*^2}{r^2} = 1 - \frac{1}{q} + \frac{\beta^2}{q^2}$$

that appears in eqs.(7), (9), (10), and (13) that positive D means that the coordinates t and r are timelike and spacelike respectively, whereas negative D means that the physical natures of the coordinates t and r are reversed. There are three different cases. (i) The case $\beta^2 > 1/4$ leads to $D > 0$ for all values of q . (ii) For $\beta^2 < 1/4$, there are two coordinate singularities occurring on the surfaces $q = q_{\pm}$ defined by

$$q_{\pm} = \frac{1}{2} \pm \left(\frac{1}{4} - \beta^2\right)^{1/2}.$$

The function D is positive for $q > q_+$ or $q < q_-$, and is negative in the region $q_- < q < q_+$. The case for $q = q_+$ can be compared to that for the Schwarzschild horizon at $q = 1$. (iii) For the case $\beta^2 = 1/4$, the function D is positive everywhere except at $q = 1/2$ where it equals zero. The coordinate q is spacelike everywhere except at $q = 1/2$ and $q = 1/2$ is an event horizon.

We now discuss how the parameter space (e^2, s^2) for a given β^2 should be divided into regions for different types of solutions of eq.(16). The discriminant Δ of the quartic equation

$$a_0U^4 + 4a_1U^3 + 6a_2U^2 + 4a_3U + a_4 = 0, \quad (24)$$

where the a'_s are given by eqs.(17)-(21), is given by

$$\Delta \equiv 27J^2 - I^3 \quad (25)$$

where

$$I = a_0a_4 - 4a_1a_3 + 3a_2^2, \quad (26)$$

and

$$J = \begin{vmatrix} a_0 & a_1 & a_2 \\ a_1 & a_2 & a_3 \\ a_2 & a_3 & a_4 \end{vmatrix}, \quad (27)$$

For the quartic equation (24), $\Delta < 0$ gives four real or four complex roots, $\Delta > 0$ gives two real and two complex roots, and $\Delta = 0$ gives repeated roots. In the Schwarzschild limit $\beta^2 = 0$, Δ reduces to $27g_3^2 - g_2^3$. Analytic expressions for the roots of a quartic equation can be written down but they are generally cumbersome and we shall not give them here. The four roots can be numerically obtained for a given set of parameters β^2 , e^2 , and s^2 , but it would be useful to know just from the given set of parameters represented by a point in the parameter space what type of trajectories one would expect.

The mathematical conditions $\Delta < 0$ and $\Delta > 0$ divide the parameter space (e^2, s^2) for a given value of β^2 into two regions which we call Regions I and II respectively, with $\Delta = 0$ forming the boundary of the two regions. The three analytic solutions representing three types of trajectories which we present below are all expressed in terms of the Jacobian elliptic functions [5] with modulus k that are analogous to those we presented in refs.3 and 4 for the Schwarzschild geometry. The first two solutions which we call Solutions (A1) and (A2) apply in Region I and the third which we call Solution (B) applies in Region II. We do not discuss the special motion along a radius for which $h = 0$ and s is infinite.

The boundary between Regions I and II given by the mathematical condition $\Delta = 0$ is represented by three curves in the (e^2, s^2) parameter space for a given specific value of β^2 which we shall refer to as the Y_0 , Y'_1 and Y_1 curves respectively. Figure 1 shows the parameter space (e^2, s^2) that exhibits part of the horizontal e^2 axis from $-\infty$ to $+\infty$ and part of the vertical s^2 axis from 0 to $+\infty$. The Y_0 curve coincides with the e^2 -axis represented by $s^2 = 0$, is the bottom line of Region I for $0 \leq e^2 \leq +\infty$, and is the bottom line of Region II for $-\infty \leq e^2 < 0$, for all values of β^2 . That is

$$Y_0 : s^2 = 0.$$

In Fig.1, the light dashed and light solid curves from V_0 are the Y'_1 and Y_1 curves for the specific value of $\beta^2 = 0$, and the heavy dashed and heavy solid curves from V_1 are the Y'_1 and Y_1 curves for the specific value of $\beta^2 = 1/4$. Region I for a specific value of β^2 is the parameter space enclosed by Y'_1 on the left, Y_1 on the top, and the e^2 -axis from 0 to $+\infty$ at the bottom. Region II is the parameter space outside of Region I above the e^2 -axis. We describe all this in greater detail below.

For a given value of β^2 , the Y'_1 curve is characterized by $\Delta = 0$ and $k^2 = 0$, where k is the modulus of the Jacobian elliptic functions used to describe the trajectories of the particle [see eqs.(34) and (46) below]. It extends from a special point that we call the vertex point $(e_v^2(\beta^2), s_v^2(\beta^2))$ to the origin $(0, 0)$ and forms the left boundary of Region I with Region II. The Y_1 curve is characterized by $\Delta = 0$ and $k^2 = 1$. It extends from $(e_v^2(\beta^2), s_v^2(\beta^2))$ to $(+\infty, 0)$ and forms the upper boundary of Region I with Region II. The vertex point is in fact the intersection point of all $k^2 = \text{const.}$ curves for $0 \leq k^2 \leq 1$ [see refs.3 and 4]. We write the Y'_1 and Y_1 curves generally as

$$\begin{aligned} Y'_1 &: s^2 = y'_1(e^2, \beta^2), \\ Y_1 &: s^2 = y_1(e^2, \beta^2), \end{aligned}$$

where y'_1 and y_1 are two specific functions of e^2 and β^2 obtained from setting the discriminant Δ given by eq.(25) of the quartic equation (24) equal to zero.

For the special value of $\beta^2 = 0$, the Schwarzschild limit, we have the simple expressions for y'_1 and y_1 [3,4]

$$s^2 = \frac{1 - 9e^2 \mp \sqrt{(1 + 3e^2)^3}}{27(1 - e^2)^2} \quad (28)$$

with the upper and lower signs for Y'_1 and Y_1 respectively. They meet and terminate at the vertex point $V_0 = (e_v^2, s_v^2) = (-1/3, 1/12)$ (see Fig.1). Equation (28) can be inverted to give e^2 in terms of s^2 as

$$e^2 = \frac{1 - 18s^2 + 54s^4 \mp \sqrt{(1 - 12s^2)^3}}{54s^4}, \quad (29)$$

For the special value of $\beta^2 = 1/4$, we have the following simple expressions for y'_1 and y_1 :

$$s^2 = \frac{1 - 12e^2 \mp \sqrt{(1 + 4e^2)^3}}{2(3 - 4e^2)^2} \quad (30)$$

with the upper and lower signs for Y'_1 and Y_1 respectively. They meet and terminate at the vertex point $V_1 = (e_v^2, s_v^2) = (-1/4, 1/8)$ (see Fig.1). Equation (30) can be inverted to give e^2 in terms of s^2 as

$$e^2 = \frac{1 - 12s^2 + 24s^4 \mp \sqrt{(1 - 8s^2)^3}}{32s^4}. \quad (31)$$

We shall refer to Y'_1 and Y_1 as the left and upper boundaries respectively of Region I with Region II. The intersection point of Y'_1 and Y_1 is the vertex point where the innermost stable circular orbit (ISCO) occurs (see the following section).

The left and upper boundary curves of Region I with Region II for the intermediate values of $0 < \beta^2 < 1/4$ are between these two cases and can be put in place approximately. The points on the curves Y'_1 and Y_1 will be referred to as $(e_1'^2, s_1'^2)$ and (e_1^2, s_1^2) respectively.

The vertex points for various values of β^2 can be conveniently obtained numerically from setting $I = J = 0$ from eqs.(26) and (27), and some of these are given in the following table.

β^2	$e_v^2(\beta^2)$	$s_v^2(\beta^2)$
0.25	-0.250000	0.125000
0.20	-0.267596	0.111453
0.15	-0.285240	0.101821
0.10	-0.302119	0.094384
0.05	-0.318135	0.088363
0	-0.333333	0.083333

Another "boundary" curve of interest is one that represents the total energy equal to zero, or $\kappa^2 = 0$ which in our (e^2, s^2) parameter space is represented by the curve $s^2(1 - e^2) = 1$, or

$$Y_2 : s^2 = \frac{1}{1 - e^2}. \quad (32)$$

We shall refer to this curve as Y_2 [not shown in Fig.1] and refer to eq.(32) as $s^2 = y_2(e^2)$ that applies to any value of β^2 as the top boundary of Region II. The points on this boundary will be referred to as (e_2^2, s_2^2) . The physical requirement that $\kappa^2 \geq 0$, where κ is given by eq.(12), leads to the condition that $s^2 \leq 1/(1 - e^2)$. We call the region $s^2 > s_2^2$ Region II'.

The analytic solutions that we shall present for the R-N geometry, in analogy with those we presented in refs.3 and 4 for the Schwarzschild geometry, are given in three forms which we call Solution (A1), Solution (A2) and Solution (B); the first two apply in Region I and the third applies in Region II. When $\Delta \leq 0$, the four real roots of the quartic equation (24) are arranged in the order $\varepsilon_1 > \varepsilon_2 > \varepsilon_3 > \varepsilon_4$. All analytic solutions of eq.(16) are expressed in terms of the Jacobian elliptic functions [5] which become circular or hyperbolic functions for special cases.

Solution (A1) For $\Delta \leq 0$, $\varepsilon_1 > \varepsilon_2 > \varepsilon_3 \geq U > \varepsilon_4$ Applicable in Region I

Writing the right-hand side of eq.(16) as $16\beta^2(\varepsilon_1 - U)(\varepsilon_2 - U)(\varepsilon_3 - U)(U - \varepsilon_4)$, we find the equation for the trajectory to be

$$\frac{1}{q} = \frac{1}{3} + 4 \frac{\varepsilon_4(\varepsilon_1 - \varepsilon_3) + \varepsilon_1(\varepsilon_3 - \varepsilon_4)sn^2(\gamma\phi, k)}{(\varepsilon_1 - \varepsilon_3) + (\varepsilon_3 - \varepsilon_4)sn^2(\gamma\phi, k)}, \quad (33)$$

where the modulus k of the elliptic functions is given by

$$k^2 = \frac{(\varepsilon_1 - \varepsilon_2)(\varepsilon_3 - \varepsilon_4)}{(\varepsilon_1 - \varepsilon_3)(\varepsilon_2 - \varepsilon_4)}, \quad (34)$$

and

$$\gamma = 2\beta\sqrt{(\varepsilon_1 - \varepsilon_3)(\varepsilon_2 - \varepsilon_4)}. \quad (35)$$

The modulus k has a range $0 \leq k^2 \leq 1$. For $k^2 = 0$, $sn(x, 0) = \sin x$, and for $k^2 = 1$, $sn(x, 1) = \tanh x$.

For the bound orbits of the elliptic-type in Region I confined to $e^2 < 1$, ε_4 is greater than $-1/12$, and the initial point at $\phi = 0$ of the bound orbit has been chosen so that the dimensionless distance q of the particle from the black hole

is given by $1/q = 1/q_{\max} = 1/3 + 4\varepsilon_4$, where q_{\max} is the maximum distance of the particle from the black hole. The minimum distance q_{\min} of the particle from the black hole is given by $1/q_{\min} = 1/3 + 4\varepsilon_3$. The geometric eccentricity can be defined in terms of q_{\max} and q_{\min} by $(q_{\max} - q_{\min})/(q_{\max} + q_{\min})$. The precessional angle $\Delta\phi$ is given by

$$\Delta\phi = \frac{2K(k)}{\gamma} - 2\pi, \quad (36)$$

where $K(k)$ is the complete elliptic integral of the first kind. For the unbound parabolic-type orbits characterized by $e^2 = 1$ in Region I, $\varepsilon_4 = -1/12$, and for the unbound hyperbolic-type orbits characterized by $e^2 > 1$ in Region I, $\varepsilon_4 < -1/12$, the particle comes from infinity from a polar angle Ψ_1 given by

$$\Psi_1 = \gamma^{-1} sn^{-1} \left(\sqrt{-\frac{(\varepsilon_1 - \varepsilon_3)(1 + 12\varepsilon_4)}{(\varepsilon_3 - \varepsilon_4)(1 + 12\varepsilon_1)}}, k \right), \quad (37)$$

and returns to infinity at a polar angle Ψ'_1 given by

$$\Psi'_1 = \frac{2K}{\gamma} - \Psi_1, \quad (38)$$

Equation (37) is obtained from eq.(33) by setting $q = \infty$. The deflection angle Θ can be defined as

$$\Theta \equiv \Psi'_1 - \Psi_1 - \pi. \quad (39)$$

Solution (A2) For $\Delta \leq 0$, $\varepsilon_1 > U > \varepsilon_2 > \varepsilon_3 > \varepsilon_4$ Applicable in Region I

Writing the right-hand side of eq.(16) as $16\beta^2(\varepsilon_1 - U)(U - \varepsilon_2)(U - \varepsilon_3)(U - \varepsilon_4)$, we find the equation for the trajectory to be

$$\frac{1}{q} = \frac{1}{3} + 4 \frac{\varepsilon_2(\varepsilon_1 - \varepsilon_3) - \varepsilon_3(\varepsilon_1 - \varepsilon_2)sn^2(\gamma\phi, k)}{(\varepsilon_1 - \varepsilon_3) - (\varepsilon_1 - \varepsilon_2)sn^2(\gamma\phi, k)}, \quad (40)$$

where k and γ are given by the same eqs.(34) and (35). The initial distance q_0 of the particle from the black hole at $\phi = 0$ has been chosen to be given by $1/q_0 = 1/3 + 4\varepsilon_2$. It is clear that q_0 is less than q_{\min} given by Solution (A1) at any given point inside Region I.

Solution (B) For $\Delta > 0$, $\varepsilon_1 \geq U > \varepsilon_2$, and $\varepsilon_3, \bar{\varepsilon}_3$ complex, where $\varepsilon_1, \varepsilon_2, \varepsilon_3$ and $\bar{\varepsilon}_3$ are the roots of the quartic equation (24).

This Solution is applicable in Region II.

Writing the right-hand side of eq.(16) as $16\beta^2(\varepsilon_1 - U)(U - \varepsilon_2)(U - \varepsilon_3)(U - \bar{\varepsilon}_3)$, we find the equation for the trajectory to be

$$\frac{1}{q} = \frac{1}{3} + 4 \frac{\varepsilon_2 A(1 + cn(2\gamma\phi, k)) + \varepsilon_1 B(1 - cn(2\gamma\phi, k))}{A(1 + cn(2\gamma\phi, k)) + B(1 - cn(2\gamma\phi, k))}, \quad (41)$$

where

$$A^2 = (\varepsilon_1 - b_1)^2 + a_1^2, \quad (42)$$

$$B^2 = (\varepsilon_2 - b_1)^2 + a_1^2, \quad (43)$$

$$a_1^2 = -\frac{(\varepsilon_3 - \bar{\varepsilon}_3)^2}{4}, \quad (44)$$

$$b_1 = \frac{\varepsilon_3 + \bar{\varepsilon}_3}{2}, \quad (45)$$

$$k^2 = \frac{(\varepsilon_1 - \varepsilon_2)^2 - (A - B)^2}{4AB}, \quad (46)$$

and

$$\gamma = 2\beta\sqrt{AB}. \quad (47)$$

For $k^2 = 0$, $cn(x, 0) = \cos x$, and for $k^2 = 1$, $cn(x, 1) = \sec hx$. For $e^2 < 1$ in Region II, ε_2 is greater than $-1/12$. The initial distance q at $\phi = 0$ of the particle from the black hole has been chosen to be given by $1/q_0 = 1/3 + \varepsilon_2$. For $e^2 \geq 1$ in Region II, ε_2 is $\leq -1/12$, the particle comes from infinity at a polar angle Φ_2 given by

$$\Phi_2 = (2\gamma)^{-1} cn^{-1} \left(-\frac{(1 + 12\varepsilon_2)A + (1 + 12\varepsilon_1)B}{(1 + 12\varepsilon_2)A - (1 + 12\varepsilon_1)B}, k \right), \quad (48)$$

and returns to infinity at a polar angle Φ'_2 given by

$$\Phi'_2 = \frac{2K}{\gamma} - \Phi_2. \quad (49)$$

In all three Solutions above, the Schwarzschild limit is obtained if we let $\beta \rightarrow 0$, $\varepsilon_1 \rightarrow \infty$, such that $2\beta\sqrt{\varepsilon_1} \rightarrow 1$.

3 Examples of the Particle Trajectories Including Special Cases

Region I ($\Delta \leq 0$) allows two types of trajectory, given by Solutions (A1) and (A2) respectively, depending on the initial distance of the particle from the black hole. Solution (A1) expressed by eq.(33) gives trajectories that are similar to those for the Schwarzschild geometry which we classify into three types: the elliptic type ($e_1'^2 \leq e^2 < 1$), the parabolic type ($e^2 = 1$) and the hyperbolic type ($e^2 > 1$) [4, 20].

Figures 2-5 show some examples of trajectories of an electrically neutral particle when q is plotted versus ϕ . These trajectories are given by eqs.(33), (40) and (41) where the electrically charged black hole is located at the origin.

Figure 2 shows an example of a precessing elliptic-type orbit in Region I given by eq.(33) for $e^2 = 1/4$, $s^2 = 0.037725$, and $\beta^2 = 1/4$ for which the precession angle $\Delta\phi$ given by eq.(36) is 43.0° . Comparing this with the elliptic-type orbit

at the same point (e^2, s^2) for the case $\beta^2 = 0$ (the Schwarzschild limit) for which $\Delta\phi = 60.5^\circ$ [3, Fig.5], we see that the presence of electric charge on the black hole reduces the precession angle $\Delta\phi$.

Figure 3 shows an example of a hyperbolic-type orbit in Region I given by eq.(33) for $e^2 = 4$, $s^2 = 0.029564$, and $\beta^2 = 1/4$ for which the deflection angle Θ given by eq.(39) is 101.1° . Comparing this with the hyperbolic-type orbit at the same point (e^2, s^2) for the case $\beta^2 = 0$ for which $\Theta = 115.6^\circ$ [20, Fig.3], we see that the presence of electric charge on the black hole reduces the deflection angle Θ .

The presence of electric charge on the black hole makes a greater difference to the trajectories given by eq.(40) of Solution (A2) in Region I and to those given by eq.(41) of Solution (B) in Region II. It changes a terminating orbit into a "wandering" orbit in which the particle wanders around the black hole as its distance q from the black hole oscillates between $1/\varepsilon_2$ and $1/\varepsilon_1$. Figure 4 shows an example of a wandering orbit in Region I given by eq.(40) for $e^2 = 1/4$, $s^2 = 0.0319276$ and $\beta^2 = 0.1$ for which $q_+ = 0.88730$ and $q_- = 0.11270$. The trajectory, starting at a distance $q_0 = 1.0178$ enters a region between q_+ and q_- and does not terminate at the center of the black hole but instead it wanders around the center of the black hole. The physical significance of the trajectory in the region $q_- < q < q_+$ is not completely clear [1,2]. Compare this with the terminating orbit for the case $\beta^2 = 0$ [3, Fig.6(b)].

Figure 5 shows an example of a wandering orbit given by eq.(41) in Region II for $e^2 = 4$, $s^2 = 0.040$ and $\beta^2 = 1/4$. The particle comes from infinity at an angle of 55.3° and instead of terminating at the black hole as for the case of $\beta^2 = 0$, it swirls around the black hole and goes to infinity at an angle of 754.6° . It, however, goes through a region of $q < q_+ = q_- = 0.5$ to a minimum distance of $q_{\min} = 0.3965$ the physical significance of which is not clear, and thus the part of the trajectory going back to infinity may not be physically realized.

The wandering orbits given by eqs.(40) and (41) become terminating orbits in the Schwarzschild limit $\beta \rightarrow 0$, $\varepsilon_1 \rightarrow \infty$ such that $2\beta\sqrt{\varepsilon_1} \rightarrow 1$.

The boundaries Y_0 , Y'_1 and Y_1 represent the special case $\Delta = 0$ on which the particle trajectories are of special types [see Fig.1 and the description given by eqs.(28)-(31)].

On Y_0 , we have $s^2 = 0$. The quartic equation (24) becomes

$$-\left(U + \frac{1}{12}\right)^2 \left[16\beta^2 U^2 - \frac{4}{3}(-2\beta^2 + 3)U + \frac{1}{9}(\beta^2 + 6) \right] = 0$$

which, for $0 \leq \beta^2 \leq 1/4$, has four real roots given by

$$\begin{aligned} \varepsilon_1 &= \frac{1}{24} \frac{-2\beta^2 + 3 + 3\sqrt{1 - 4\beta^2}}{\beta^2}, \\ \varepsilon_2 &= \frac{1}{24} \frac{-2\beta^2 + 3 - 3\sqrt{1 - 4\beta^2}}{\beta^2}, \\ \varepsilon_3 &= \varepsilon_4 = -\frac{1}{12}. \end{aligned}$$

The trajectory of the particle is given from eq.(33) by $1/q = 0$ or $q = \infty$, i.e. the particle is infinitely far away from the black hole and its trajectory is a straight line independent of β^2 . From eq.(34), the curve Y_0 is also characterized by $k^2 = 0$.

On the left boundary Y_1' (or $s_1'^2$) of Region I, we have $\varepsilon_3 = \varepsilon_4$ and $k^2 = 0$, the elliptic-type orbits given by Solution (A1) become stable circular orbits with radii q_c given by

$$\frac{1}{q_c} = \frac{1}{3} + 4\varepsilon_4, \quad (50)$$

whereas the wandering orbits given by Solution (A2) continue to be wandering orbits given by

$$\frac{1}{q} = \frac{1}{3} + 4 \frac{\varepsilon_2(\varepsilon_1 - \varepsilon_3) - \varepsilon_3(\varepsilon_1 - \varepsilon_2) \sin^2(\gamma\phi)}{(\varepsilon_1 - \varepsilon_3) - (\varepsilon_1 - \varepsilon_2) \sin^2(\gamma\phi)}. \quad (51)$$

On the upper boundary Y_1 (or s_1^2) of Region I where $\varepsilon_2 = \varepsilon_3$ and $k^2 = 1$, the elliptic-, parabolic- and hyperbolic-type orbits given by Solution (A1) and the wandering orbits given by Solution (A2) all become unstable asymptotic circular orbits with radii q_u given by

$$\frac{1}{q_u} = \frac{1}{3} + 4\varepsilon_3. \quad (52)$$

The intersection of Y_1' and Y_1 in the parameter space is the vertex point V where $\varepsilon_1 = \varepsilon_2 = \varepsilon_3$ and where the innermost stable circular orbit (ISCO) occurs. For the Schwarzschild geometry ($\beta^2 = 0$), V is at $(e^2, s^2) = (-1/3, 1/12)$ or $(\kappa^2, s^2) = (8/9, 1/12)$ shown as V_0 in Fig.1, and the radius of ISCO is $q_c = 3$ or $r_c = 6GM/c^2$. For the R-N geometry at the special value of $\beta^2 = 1/4$, V is at $(e^2, s^2) = (-1/4, 1/8)$ or $(\kappa^2, s^2) = (27/32, 1/8)$ [21] shown as V_1 in Fig.1, and the radius of ISCO is $q_c = 2$ or $r_c = 4GM/c^2$.

The upper boundary Y_2 of Region II is characterized by zero total energy or $\kappa^2 = 0$. The quartic equation (24) becomes

$$-\left(U^2 + \frac{1}{6}U + \frac{1}{12^2} + \frac{1}{4}s^2\right) \left[16\beta^2 U^2 + \frac{4}{3}(2\beta^2 - 3)U + \frac{1}{9}(\beta^2 + 6)\right] = 0$$

which, for $0 \leq \beta^2 \leq 1/4$, has four roots given by

$$\begin{aligned} \varepsilon_1 &= \frac{1}{24} \frac{-2\beta^2 + 3 + 3\sqrt{1 - 4\beta^2}}{\beta^2}, \\ \varepsilon_2 &= \frac{1}{24} \frac{-2\beta^2 + 3 - 3\sqrt{1 - 4\beta^2}}{\beta^2}, \\ \varepsilon_3 &= -\frac{1}{12} + \frac{1}{2}is, \\ \bar{\varepsilon}_3 &= -\frac{1}{12} - \frac{1}{2}is, \end{aligned}$$

where β^2 is assumed to be $\leq 1/4$. The trajectory is given by eq.(41) with k^2 and γ given by

$$\begin{aligned} k^2 &= \frac{1}{2} - \frac{1}{2} \frac{1 + 4\beta^2 s^2}{[1 + 4(1 - 2\beta^2)s^2 + 16\beta^4 s^4]^{1/2}}, \\ \gamma &= \frac{1}{2} [1 + 4(1 - 2\beta^2)s^2 + 16\beta^4 s^4]^{1/4}. \end{aligned}$$

The initial distance q_0 of the particle from the black hole at $\phi = 0$ is given by $1/q_0 = 1/3 + 4\varepsilon_2$ which yields

$$q_0 = \frac{1}{2} \left(1 + \sqrt{1 - 4\beta^2} \right)$$

which is the distance q_+ of the outer horizon from the black hole. Thus all particle trajectories on Y_2 start from the horizon (in a direction perpendicular to the line joining it to the center of the black hole).

4 Light Trajectories in the R-N Geometry

The trajectory of a photon is a null geodesic. Instead of using the proper time τ as a parameter, we use some affine parameter σ along the geodesic. Considering motion in the equatorial plane, the equations of motion in the R-N geometry are given by

$$\left(1 - \frac{\alpha}{r} + \frac{Q_*^2}{r^2} \right) \dot{t} = \kappa, \quad (53)$$

$$c^2 \left(1 - \frac{\alpha}{r} + \frac{Q_*^2}{r^2} \right) \dot{t}^2 - \left(1 - \frac{\alpha}{r} + \frac{Q_*^2}{r^2} \right)^{-1} \dot{r}^2 - r^2 \dot{\phi}^2 = 0, \quad (54)$$

$$r^2 \dot{\phi} = h, \quad (55)$$

where the derivative $\dot{}$ represents $d/d\sigma$. The analog of eq.(13) is

$$\dot{r}^2 + \frac{h^2}{r^2} \left(1 - \frac{\alpha}{r} + \frac{Q_*^2}{r^2} \right) = c^2 \kappa^2. \quad (56)$$

Substituting $dr/d\sigma = (dr/d\phi)(d\phi/d\sigma) = (h/r^2)(dr/d\phi)$ into the combined energy equation above gives the differential equation for the trajectory of light

$$\left(\frac{du}{d\phi} \right)^2 = -Q_*^2 u^4 + \alpha u^3 - u^2 + \frac{c^2 \kappa^2}{h^2}, \quad (57)$$

where $u = 1/r$. We define the dimensionless inverse distance U by

$$U = \frac{1}{q} \equiv \frac{\alpha}{r} = \alpha u. \quad (58)$$

In terms of U , eq.(57) becomes

$$\left(\frac{dU}{d\phi}\right)^2 = -\beta^2 U^4 + U^3 - U^2 + \frac{c^2 \kappa^2 \alpha^2}{h^2}, \quad (59)$$

where β^2 is defined by eq.(6) as before, but U is defined somewhat differently from eq.(15). We note that the trajectory depends on the ratio κ/h (and β) and not on κ and h separately [19]. We could use the four roots of the quartic equation

$$-\beta^2 U^4 + U^3 - U^2 + \frac{c^2 \kappa^2 \alpha^2}{h^2} = 0 \quad (60)$$

obtained numerically from the given set of parameters β^2 and κ/h for characterizing the trajectory. Instead, as we did in a similar fashion in ref.3, we replace κ/h by an alternative parameter as follows. Let R denote the distance of the light beam to the center of the black hole when the trajectory of the light beam is such that $dU/d\phi = 0$. When a light beam is simply deflected by the presence of the charged black hole, R is the closest distance of the light beam to the black hole and may be unique; but for a more general trajectory it may not be unique. We let $U_1 = R/\alpha$ denote the value of U at which $dU/d\phi = 0$. Then we can replace $c^2 \kappa^2 \alpha^2 / h^2$ by $\beta^2 U_1^4 - U_1^3 + U_1^2$ and write eq.(59) as

$$\left(\frac{dU}{d\phi}\right)^2 = -\beta^2 U^4 + U^3 - U^2 + \beta^2 U_1^4 - U_1^3 + U_1^2. \quad (61)$$

We do not discuss the special case when the light is along a path that is directly toward the black hole. The advantage of using eq.(61) is that one root $U = U_1$ of the quartic equation (60) is assumed known or given physically, and the other three roots of the resulting cubic equation

$$U^3 + a_1 U^2 + a_2 U + a_3 = 0 \quad (62)$$

where

$$a_1 = -(\beta^{-2} - U_1), \quad (63)$$

$$a_2 = (1 - U_1)\beta^{-2} + U_1^2, \quad (64)$$

$$a_3 = [(1 - U_1)\beta^{-2} + U_1^2]U_1, \quad (65)$$

can be written down analytically in rather simple expressions. Defining

$$a = -\frac{\beta^{-4}}{3} \left\{ 1 - (3 - U_1)\beta^2 - 2U_1^2\beta^4 \right\}, \quad (66)$$

$$b = -\frac{2\beta^{-6}}{27} \left\{ 1 - \frac{3(3 - U_1)}{2}\beta^2 - \frac{3(6U_1 - 5U_1^2)}{2}\beta^4 - 10U_1^3\beta^6 \right\}, \quad (67)$$

the discriminant Δ of the cubic equation (62) is given by

$$\Delta = \frac{b^2}{4} + \frac{a^3}{27},$$

or

$$\Delta = -\frac{\beta^{-8}}{2^2 \cdot 3^3} \left\{ \begin{array}{l} (1 + 2U_1 - 3U_1^2) - 2(2 + 4U_1 - 9U_1^2 + U_1^3)\beta^2 \\ -(20 - 12U_1 + 3U_1^2)U_1^2\beta^4 - 8(4 - 3U_1)U_1^4\beta^6 - 16U_1^6\beta^8 \end{array} \right\}. \quad (68)$$

For $\Delta \leq 0$, the cubic equation (62) has three real roots. We define

$$\cos \theta = -\frac{b}{2\sqrt{-\frac{a^3}{27}}}. \quad (69)$$

The three real roots of the cubic equation (62) are given by

$$x_1 = 2\sqrt{\frac{-a}{3}} \cos \frac{\theta}{3} + \frac{1}{3}(\beta^{-2} - U_1), \quad (70)$$

$$x_2 = 2\sqrt{\frac{-a}{3}} \cos \frac{\theta + 4\pi}{3} + \frac{1}{3}(\beta^{-2} - U_1), \quad (71)$$

$$x_3 = 2\sqrt{\frac{-a}{3}} \cos \frac{\theta + 2\pi}{3} + \frac{1}{3}(\beta^{-2} - U_1). \quad (72)$$

For $\Delta > 0$, the cubic equation (62) has one real and two complex roots given by

$$x_1 = \left(-\frac{b}{2} + \sqrt{\Delta}\right)^{1/3} + \left(-\frac{b}{2} - \sqrt{\Delta}\right)^{1/3} + \frac{1}{3}(\beta^{-2} - U_1), \quad (73)$$

$$x_2 = \omega \left(-\frac{b}{2} + \sqrt{\Delta}\right)^{1/3} + \omega^2 \left(-\frac{b}{2} - \sqrt{\Delta}\right)^{1/3} + \frac{1}{3}(\beta^{-2} - U_1), \quad (74)$$

$$x_3 = \bar{\omega} \left(-\frac{b}{2} + \sqrt{\Delta}\right)^{1/3} + \omega \left(-\frac{b}{2} - \sqrt{\Delta}\right)^{1/3} + \frac{1}{3}(\beta^{-2} - U_1), \quad (75)$$

where $\omega = -1/2 + i\sqrt{3}/2$ and $\bar{\omega} = -1/2 - i\sqrt{3}/2$.

For the Schwarzschild geometry, the single parameter U_1 can be used to characterize the trajectory of light, and there are three regions: Region I for $0 \leq U_1 \leq 2/3$ ($\infty > R \geq 3GM/c^2$), Region II for $2/3 < U_1 \leq 1$ ($3GM/c^2 > R \geq 2GM/c^2$), and Region III for $1 < U_1 \leq \infty$ ($2GM/c^2 > R \geq 0$).

For the R-N geometry, the parameter space (U_1, β^2) can be divided also into basically three regions as shown in Fig.6. The mathematical condition $\Delta = 0$ produces three curves which we call y_1, y_2 and y_3 .

$$y_1 : \beta^2 = \frac{1}{12U_1^2} \left(f + \frac{19U_1^2 - 52U_1 + 4}{f} + 2U_1 - 4 \right), \quad (76)$$

where

$$f = \left\{ \frac{3\sqrt{6U_1} (729U_1^5 - 486U_1^4 - 54U_1^3 + 1144U_1^2 + 736U_1 + 128)^{1/2}}{+215U_1^3 - 192U_1^2 + 276U_1 + 8} \right\}^{1/3}; \quad (77)$$

$$y_2 : \beta^2 = \frac{3U_1 - 2}{4U_1^2}; \quad (78)$$

$$y_3 : \beta^2 = \frac{1}{U_1} - \frac{1}{U_1^2}; \quad (79)$$

and they are shown in Fig.6. The curves y_1 and y_2 touch at what we call the vertex point V the coordinates of which are given by $(4/3, 9/32) = (1.33333, 0.28125)$. The curves y_2 and y_3 intersect at $(2, 1/4)$.

Region I is the parameter space bounded by the β^2 -axis on the left, by y_1 on the top [between $(0, 1/4)$ and V], and by y_2 on the right [between $(2/3, 0)$ and V]. Region II is the parameter space bounded by y_2 on the left [between $(2/3, 0)$ and V], by y_3 on the right [between $(1, 0)$ and $(+\infty, 0)$], and by y_1 at the top [between V and $(+\infty, 0)$]. Region II is divided into two parts IIA and IIB by the curve y_2 between V and $(2, 1/4)$. Region III is the parameter space under the curve y_3 , and it is divided into two parts IIIA and IIIB by the curve y_2 from $(2, 1/4)$ to $(+\infty, 0)$.

The analytic solutions that we shall present for the trajectory of light in the R-N geometry, in analogy with those we presented in ref.3 for the Schwarzschild geometry, are given in three forms for Regions I, II and III respectively. The four roots of the quartic equation (60) consist of one real root U_1 and three roots of the cubic equation (62). When Δ given by eq.(68) is ≤ 0 , the four real roots are arranged in the order $\varepsilon_1 > \varepsilon_2 > \varepsilon_3 > \varepsilon_4$, and we shall identify the four ε 's with U_1 and the x 's given by eqs.(70)-(72) later. When Δ given by eq.(68) is > 0 , there are two real roots U_1 and x_1 , and two complex roots x_2 and \bar{x}_2 given by eqs.(73)-(75).

Solution (I) For Region I $\Delta \leq 0$, $\varepsilon_1 > \varepsilon_2 > \varepsilon_3 \geq U > \varepsilon_4$. Here we set $\varepsilon_1 = x_1$, $\varepsilon_2 = x_2$, $\varepsilon_3 = U_1$, $\varepsilon_4 = x_3$ from eqs.(70)-(72).

Writing the right-hand side of eq.(61) as $\beta^2(\varepsilon_1 - U)(\varepsilon_2 - U)(\varepsilon_3 - U)(U - \varepsilon_4)$, we find the equation for the trajectory to be

$$\frac{1}{q} = \frac{\varepsilon_3(\varepsilon_2 - \varepsilon_4) - \varepsilon_2(\varepsilon_3 - \varepsilon_4)sn^2(\gamma\phi, k)}{(\varepsilon_2 - \varepsilon_4) - (\varepsilon_3 - \varepsilon_4)sn^2(\gamma\phi, k)}, \quad (80)$$

where the modulus k of the elliptic functions is given by

$$k^2 = \frac{(\varepsilon_1 - \varepsilon_2)(\varepsilon_3 - \varepsilon_4)}{(\varepsilon_1 - \varepsilon_3)(\varepsilon_2 - \varepsilon_4)}, \quad (81)$$

and

$$\gamma = \frac{1}{2}\beta\sqrt{(\varepsilon_1 - \varepsilon_3)(\varepsilon_2 - \varepsilon_4)}. \quad (82)$$

Setting $U = 0$ and $\phi = \pi/2 + \Delta\phi/2$, where $\Delta\phi$ is the total angle of deflection of the light beam [3], we find

$$sn^2\left[\gamma\left(\frac{\pi}{2} + \frac{\Delta\phi}{2}\right), k\right] = \frac{(\varepsilon_2 - \varepsilon_4)\varepsilon_3}{(\varepsilon_3 - \varepsilon_4)\varepsilon_2}, \quad (83)$$

or

$$\Delta\phi = -\pi + \frac{2}{\gamma}sn^{-1}(\psi, k), \quad (84)$$

where

$$\psi = \sqrt{\frac{(\varepsilon_2 - \varepsilon_4)\varepsilon_3}{(\varepsilon_3 - \varepsilon_4)\varepsilon_2}}. \quad (85)$$

Solution (II) For Region II $\Delta \leq 0$, $\varepsilon_1 \geq U > \varepsilon_2 > \varepsilon_3 > \varepsilon_4$. Write the right-hand side of eq.(61) as $\beta^2(\varepsilon_1 - U)(U - \varepsilon_2)(U - \varepsilon_3)(U - \varepsilon_4)$.

For Region IIA bounded by y_2 [between $(2/3, 0)$ and $(2, 1/4)$] and y_3 [between $(1, 0)$ and $(2, 1/4)$], we set $\varepsilon_1 = x_1$, $\varepsilon_2 = U_1$, $\varepsilon_3 = x_2$, $\varepsilon_4 = x_3$ from eqs.(70)-(72). We find the equation for the trajectory to be

$$\frac{1}{q} = \frac{\varepsilon_2(\varepsilon_1 - \varepsilon_3) - \varepsilon_3(\varepsilon_1 - \varepsilon_2)sn^2(\gamma\phi, k)}{(\varepsilon_1 - \varepsilon_3) - (\varepsilon_1 - \varepsilon_2)sn^2(\gamma\phi, k)}, \quad (86)$$

where k and γ are given by the same eqs.(81) and (82), and where we have chosen the initial value of q at $\phi = 0$ to be given by $1/q = \varepsilon_2$.

For Region IIB bounded by y_2 [between V and $(2, 1/4)$], y_3 [between $(2, 1/4)$ and $(+\infty, 0)$], and y_1 [between V and $(+\infty, 0)$], we set $\varepsilon_1 = U_1$, $\varepsilon_2 = x_1$, $\varepsilon_3 = x_2$, $\varepsilon_4 = x_3$ from eqs.(70)-(72). We find the same equation for the trajectory as that given by eq.(86), or if we choose the initial value at $\phi = 0$ for q to be $1/q = \varepsilon_1$, we have the following trajectory

$$\frac{1}{q} = \frac{\varepsilon_1(\varepsilon_2 - \varepsilon_4) + \varepsilon_4(\varepsilon_1 - \varepsilon_2)sn^2(\gamma\phi, k)}{(\varepsilon_2 - \varepsilon_4) + (\varepsilon_1 - \varepsilon_2)sn^2(\gamma\phi, k)}. \quad (87)$$

The two expressions for the trajectory given by eqs.(86) and (87) are related by a coordinate rotation.

Solution (III) For Region III For $\Delta > 0$, $\varepsilon_1 \geq U > \varepsilon_2$, and $\varepsilon_3, \bar{\varepsilon}_3$ complex. Write the right-hand side of eq.(61) as $\beta^2(\varepsilon_1 - U)(U - \varepsilon_2)(U - \varepsilon_3)(U - \bar{\varepsilon}_3)$.

For Region IIIA bounded by y_3 [between $(1, 0)$ and $(2, 1/4)$] and y_2 [between $(2, 1/4)$ and $(+\infty, 0)$], we let $\varepsilon_1 = x_1$, $\varepsilon_2 = U_1$, $\varepsilon_3 = x_2$, $\bar{\varepsilon}_3 = \bar{x}_2$ from eqs.(73)-(75). Assuming the value of q to be given by $1/q = \varepsilon_2$ at $\phi = 0$, we find the equation for the trajectory to be

$$\frac{1}{q} = \frac{\varepsilon_2 A(1 + cn(2\gamma\phi, k)) + \varepsilon_1 B(1 - cn(2\gamma\phi, k))}{A(1 + cn(2\gamma\phi, k)) + B(1 - cn(2\gamma\phi, k))}, \quad (88)$$

where

$$A^2 = (\varepsilon_1 - b_1)^2 + a_1^2, \quad (89)$$

$$B^2 = (\varepsilon_2 - b_1)^2 + a_1^2, \quad (90)$$

$$a_1^2 = -\frac{(\varepsilon_3 - \bar{\varepsilon}_3)^2}{4}, \quad (91)$$

$$b_1 = \frac{\varepsilon_3 + \bar{\varepsilon}_3}{2}, \quad (92)$$

$$k^2 = \frac{(\varepsilon_1 - \varepsilon_2)^2 - (A - B)^2}{4AB}, \quad (93)$$

and

$$\gamma = \frac{1}{2}\beta\sqrt{AB}. \quad (94)$$

For Region IIIB bounded by y_2 [between $(2, 1/4)$ and $(+\infty, 0)$] and y_3 [between $(2, 1/4)$ and $(+\infty, 0)$], we let $\varepsilon_1 = U_1$, $\varepsilon_2 = x_1$, $\varepsilon_3 = x_2$, $\bar{\varepsilon}_3 = \bar{x}_2$ from eqs.(73)-(75). We find the same equation (88) for the trajectory, or

$$\frac{1}{q} = \frac{\varepsilon_2 A(1 - cn(2\gamma\phi, k)) + \varepsilon_1 B(1 + cn(2\gamma\phi, k))}{A(1 - cn(2\gamma\phi, k)) + B(1 + cn(2\gamma\phi, k))}, \quad (95)$$

if we assume that the value of q is given by $1/q = \varepsilon_2$ at $\phi = 0$. Equation (95) is related to eq.(88) by a rotation of the coordinates.

In all the Solutions for the light trajectories above, the Schwarzschild limit is obtained if we let $\beta \rightarrow 0$, $\varepsilon_1 \rightarrow \infty$, such that $\beta\sqrt{\varepsilon_1} \rightarrow 1$.

5 Examples of Light Trajectories Including Special Cases

A light beam is bent toward the black hole in Region I ($\Delta < 0$) in the R-N geometry in a manner similar to that in the Schwarzschild geometry, and the total angle of deflection is given by eq.(84). An example of a light beam bent by a charged black hole given by eq.(80) where q is plotted versus ϕ is shown in Fig.7 where the charged black hole is centered at the origin. In this case $U_1 = 0.42922$ and $\beta^2 = 0.1$ for which $q_+ = 0.8873$, $q_- = 0.1127$, and the total angle of deflection $\Delta\phi$ is 81.4° . Comparing this with the Schwarzschild case for the same value of U_1 in which the black hole has no electric charge ($\beta^2 = 0$) for

which $\Delta\phi = 90^\circ$ [3], we see that the presence of electric charge in the black hole reduces the deflection angle of the light beam.

On the upper boundary y_1 of Region I [between $(0, 1/4)$ and V , see Fig.6], $\varepsilon_1 = \varepsilon_2$, $k^2 = 0$, the inverse distance U of the photon from the blackhole lies in the range $\varepsilon_1 = \varepsilon_2 > \varepsilon_3 \geq U > \varepsilon_4$, and the trajectory is given by

$$\frac{1}{q} = \frac{\varepsilon_3(\varepsilon_2 - \varepsilon_4) - \varepsilon_2(\varepsilon_3 - \varepsilon_4) \sin^2(\gamma\phi)}{(\varepsilon_2 - \varepsilon_4) - (\varepsilon_3 - \varepsilon_4) \sin^2(\gamma\phi)}, \quad (96)$$

where the roots of the quartic equation (60) are given by

$$\varepsilon_1 = \varepsilon_2 = \sqrt{\frac{-a}{3}} + \frac{1}{3}(\beta^{-2} - U_1), \quad (97)$$

$$\begin{aligned} \varepsilon_3 &= U_1, \\ \varepsilon_4 &= -2\sqrt{\frac{-a}{3}} + \frac{1}{3}(\beta^{-2} - U_1), \end{aligned} \quad (98)$$

where γ and a are given by eqs.(82) and (66). The trajectory of a light beam is still one that is bent and the total angle of deflection $\Delta\phi$ is given by

$$\Delta\phi = -\pi + \frac{2}{\gamma} \sin^{-1} \psi, \quad (99)$$

where

$$\psi = \sqrt{\frac{(\varepsilon_2 - \varepsilon_4)\varepsilon_3}{(\varepsilon_3 - \varepsilon_4)\varepsilon_2}}. \quad (100)$$

On the right boundary y_2 of Region I with Region II [between $(2/3, 0)$ and V , see Fig.6], $\varepsilon_2 = \varepsilon_3 = U_1$, $k^2 = 1$, the trajectories become asymptotic circles of radii q_u given by $1/q_u = U_1$.

In Region II, the light trajectories given by eq.(86) or (87) are of the wandering type an example of which is shown in Fig.8 for which $U_1 = 1$ and $\beta^2 = 0.1$, and for which $q_+ = 0.8873$ and $q_- = 0.1127$. It is seen that starting from $q_0 = 1$, the trajectory can repeatedly enter and emerge from the region in which q is between q_+ and q_- . The physical interpretation of this behavior is not clear [1,2]. For the same value of U_1 but with $\beta^2 = 0$, the trajectory would simply be one that terminates at the black hole.

On the boundary y_2 from V to $(+\infty, 0)$ [see Fig.6] between Regions IIA and IIB, and between Regions IIIA and IIIB, $\varepsilon_1 = \varepsilon_2 = U_1$, $k^2 = 0$, and the trajectories are given by circles of radii q_c given by $1/q_c = U_1$.

On the upper boundary y_1 of Region IIB [between V and $(+\infty, 0)$, see Fig.6],

$$\begin{aligned}
\varepsilon_1 &= U_1, \\
\varepsilon_2 &= \varepsilon_3 = \sqrt{\frac{-a}{3}} + \frac{1}{3}(\beta^{-2} - U_1), \\
\varepsilon_4 &= -2\sqrt{\frac{-a}{3}} + \frac{1}{3}(\beta^{-2} - U_1),
\end{aligned}$$

where a is given by eq.(66), from which $k^2 = 1$ from eq.(81). From eq.(87), where γ is given by eq.(82), the trajectories become asymptotic circles of radii q_u given by $1/q_u = \varepsilon_2$ as $\gamma\phi \rightarrow \infty$ since $sn(\gamma\phi, 1) = \tanh(\gamma\phi)$.

On the boundary y_3 between Region IIA and IIIA [between $(1, 0)$ and $(2, 1/4)$, see Fig.6], $\varepsilon_3 = \varepsilon_4 = 0$, $k^2 = 0$, and the trajectories are given by

$$\frac{1}{q} = \frac{\varepsilon_1 \varepsilon_2}{\varepsilon_1 - (\varepsilon_1 - \varepsilon_2) \sin^2(\gamma\phi)}, \quad (101)$$

where γ is given by eq.(82), and

$$\begin{aligned}
\varepsilon_1 &= \beta^{-2} - U_1, \\
\varepsilon_2 &= U_1.
\end{aligned} \quad (102)$$

On the boundary y_3 between Region IIB and IIIB [between $(2, 1/4)$ and $(+\infty, 0)$, see Fig.6], $\varepsilon_3 = \varepsilon_4 = 0$, $k^2 = 0$, the trajectories are given by

$$\frac{1}{q} = \frac{\varepsilon_1 \varepsilon_2}{\varepsilon_2 + (\varepsilon_1 - \varepsilon_2) \sin^2(\gamma\phi)}, \quad (103)$$

where γ is given by eq.(82), and

$$\begin{aligned}
\varepsilon_1 &= U_1, \\
\varepsilon_2 &= \beta^{-2} - U_1.
\end{aligned} \quad (104)$$

The trajectories given by eqs.(101) and (103) are closed curves. An example of a light trajectory given by eq.(101) is shown in Fig.9 for which $U_1 = 1.2$, $\beta^2 = 0.13889$, $q_+ = 0.83333$, $q_- = 0.16667$. The closed curve has $q_{\max} = q_+$ and $q_{\min} = q_-$. At the intersection point $(2, 1/4)$ of y_3 and y_2 on which $\varepsilon_1 = \varepsilon_2 = 2$, we have a circular orbit of radius $q_c = 1/2$ or $r_c = GM/c^2$.

At the vertex point $V = (4/3, 9/32)$, $\varepsilon_1 = \varepsilon_2 = \varepsilon_3 = U_1 = 4/3$, $\varepsilon_4 = -4/9$, $\beta^2 = 9/32 = 0.28125$, $\gamma = 0$ from eq.(82), and eqs.(80), (86) and (87) all become a circular orbit with a radius $q_c = 1/U_1 = 3/4$ or $r_c = 3GM/(2c^2)$.

6 Summary

We have characterized all trajectories of an electrically neutral particle (planet) around an electrically charged black hole in the Reissner-Nordström geometry

by three dimensionless parameters e^2 , s^2 , and β^2 defined by eqs.(1), (2) and (6), and placed them on a parameter space (e^2, s^2) shown in Fig.1 that consists of two regions, called Regions I and II, where analytic solutions for the trajectories given by eqs.(33) and (40) for Region I, and by eq.(41) for Region II, apply. Analytic expressions for the boundaries of Regions I and II for two specific values of the dimensionless charge $\beta^2 = 0$ and $1/4$ are given by eqs.(28) and (30), and the corresponding curves for the boundaries are shown in Fig.1. Examples of these particle trajectories in Regions I and II are shown in Figs.2-5. Of particular interest are the following results on the effect of the presence of a net electric charge ($\beta^2 > 0$) on the black hole compared to the case when the black hole is electrically neutral ($\beta^2 = 0$ or the Schwarzschild case): (1) the precession angle of an elliptic-type orbit decreases, (2) the deflection angle of a hyperbolic-type orbit also decreases, and (3) a wandering-type orbit replaces a terminating orbit.

We have characterized the light trajectories near a charged black hole by two dimensionless parameters U_1 and β^2 , where U_1 is defined just prior to eq.(61). The parameter space (U_1, β^2) is shown in Fig.6 and is divided into three principal Regions, called I, II and III, with Regions II and III divided into sub-regions A and B. Equations (80), (86), (87), (88), and (95) apply to Regions I, IIA, IIB, IIIA, and IIIB respectively. Figures 7, 8 and 9 show examples of a light trajectory near a charged black hole in Regions I, II and on the boundary of Regions II and III. The boundary curves separating the various regions in Fig.6 are given by eqs.(76), (78) and (79). Of particular interest are the following results on the effect of the presence of a net electric charge on the black hole compared to the case when the black hole is electrically neutral: (1) the bending of a light ray decreases, (2) a wandering-type trajectory replaces a terminating one, and (3) there are closed trajectories that are not circular.

Acknowledgements

I am very grateful to Drs. Dave Kuebel and Clark Carroll for many valuable comments, corrections and suggestions, and to Dr. Krsna Dev for valuable comments and technical help. I would also like to thank Drs. C. Lämmerzahl, L. Iorio and M. Azreg-Aïnou for drawing my attention to their work after the appearance of this paper in arXiv:1402.1756v1 [gr-qc] (2014).

References

*Electronic address: fhioe@sjfc.edu

- [1] M.P. Hobson, G. Efstathiou and A.N. Lasenby: General Relativity, Cambridge University Press, 2006, Chapters 12.
- [2] S. Chandrasekhar: The Mathematical Theory of Black Holes, Oxford University Press, 1992, Chapter 5.
- [3] F.T. Hioe and D. Kuebel, Phys. Rev. D 81, 084017 (2010).
- [4] F.T. Hioe and D. Kuebel, arXiv:1207.7041v1 (2012).
- [5] P.F. Byrd and M.D. Friedman: Handbook of Elliptic Integrals for Engineers and Scientists, 2nd Edition, Springer-Verlag, New York, 1971.

- [6] Y. Hagihara, J. Astron. Geophys. 8, 67-176 (1931).
- [7] E.T. Whittaker: A Treatise on the Analytical Dynamics of Particles and Rigid Bodies, 4th Edition, Dover, New York 1944, Chapter XV.
- [8] S. Grunau and V. Kagramanova, Phys. Rev. D 83, 044009 (2011).
- [9] E. Hackmann, V. Kagramanova, J. Kunz and C. Lämmerzahl, Phys. Rev. D 78, 124018 (2008).
- [10] D. Pugliese, H. Quevedo and R. Ruffini, Phys. Rev. D 83, 104052 (2011).
- [11] L. Iorio, Gen. Relativ. Gravit. 44, 1753 (2012).
- [12] G.W. Gibbons and M. Vyska, Class. Quantum Grav. 29, 065016 (2012).
- [13] M. Azreg-Aïnou, Phys. Rev. D 87, 024012 (2013).
- [14] A.R. Forsyth, Proc. Roy. Soc. Lond. A 97, 145 (1920).
- [15] Ref.3 studied the cases for $0 \leq e^2 \leq \infty$ only. See ref.4 for the more complete results for $-\infty \leq e^2 \leq \infty$.
- [16] C. Darwin, Proc. Roy. Soc. Lond. A249, 180 (1958), *ibid.* A263, 39 (1961).
- [17] F.T. Hioe and D. Kuebel, arXiv:1208.0260v1 (2012).
- [18] F.T. Hioe, Phys. Lett. A 373, 1506 (2009).
- [19] J.L. Martin: General Relativity, Revised Edition, Prentice Hall, New York 1996, Chapter 4.
- [20] F.T. Hioe and D. Kuebel, arXiv:1008.1964v1 (2010).
- [21] C.E. Carroll obtained this result independently, private communication.

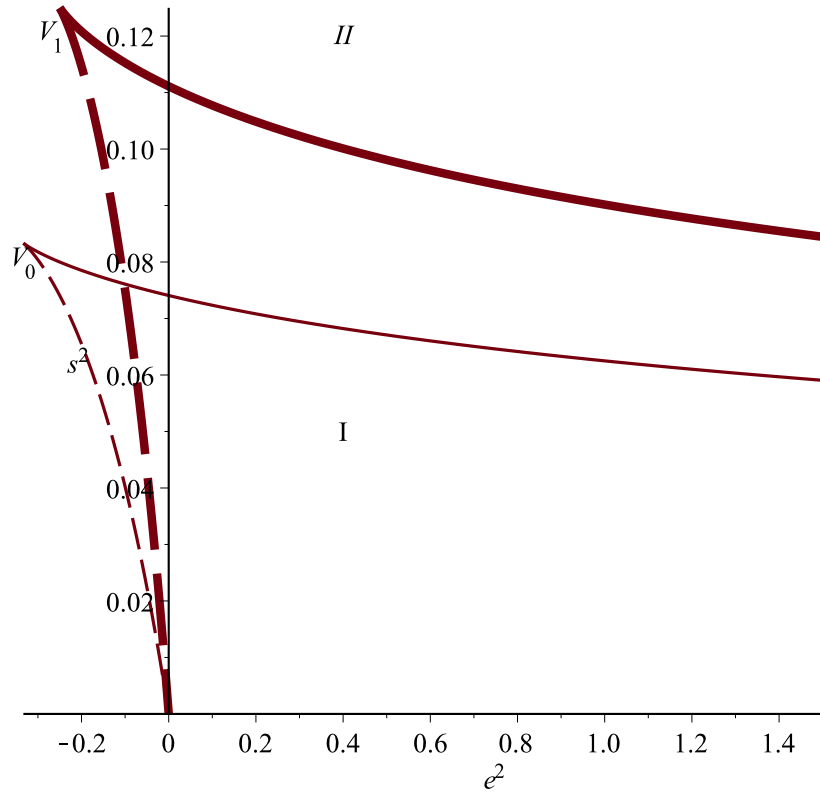


Fig.1 Boundaries of Regions I and II for Particle Trajectories.

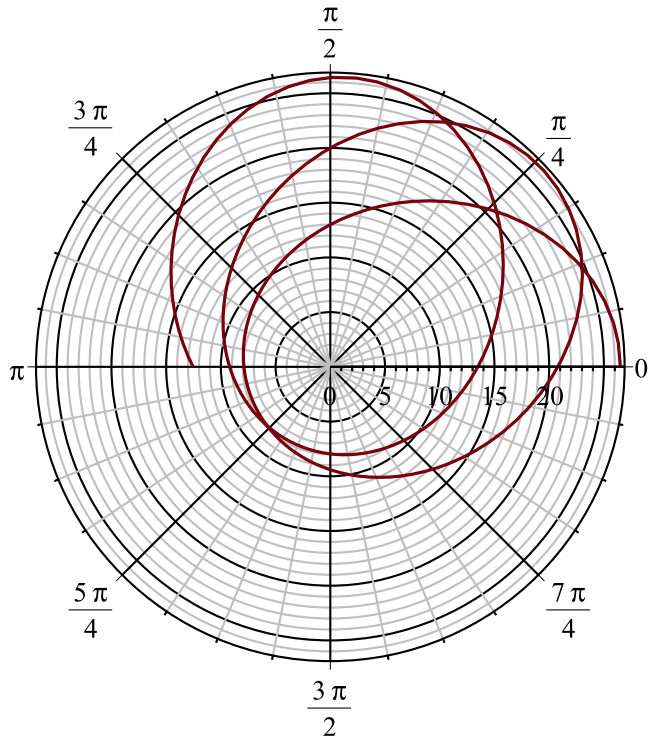


Fig.2 Elliptic-Type Particle Orbit in Region I for $e^2=0.25$, $s^2=0.037725$,
 $\beta^2=0.25$, $\Delta\phi=43.0$ deg

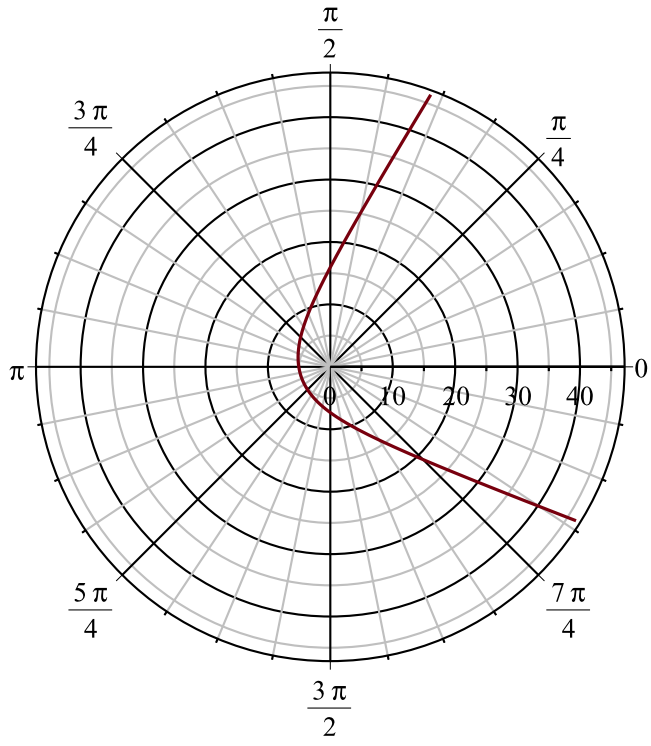


Fig.3 Hyperbolic-Type Particle Orbit in Region I for $e^2=4$, $s^2=0.029564$,
 $\beta^2=0.25$, $\Theta=101.1\text{deg}$

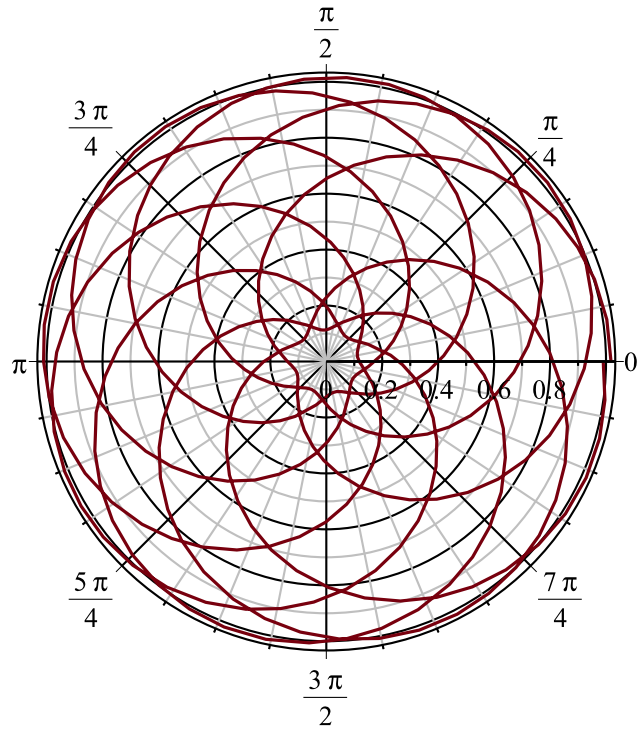


Fig.4 Wandering Particle Orbit in Region I for $e^2=0.25$, $s^2=0.0319276$,
 $\beta^2=0.1$, $q_+=0.88730$, $q_-=0.11270$, $q_0=1.0178$

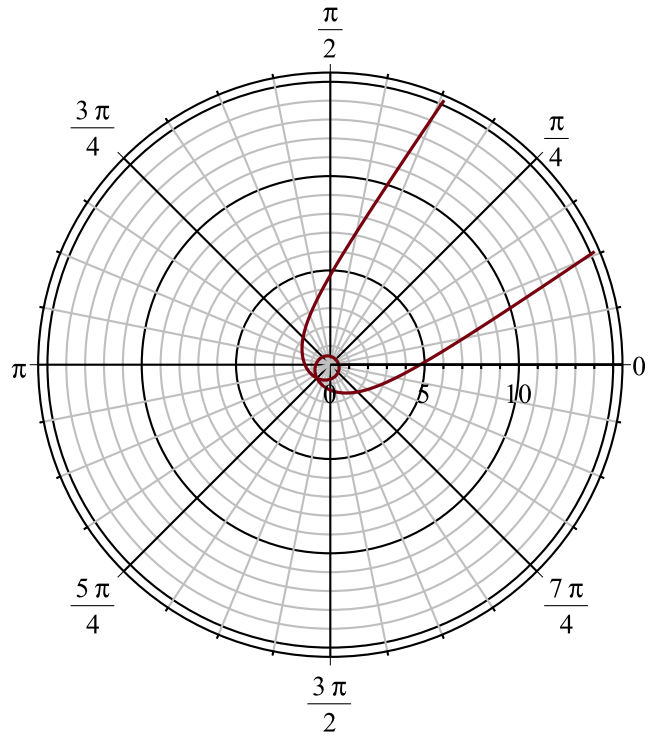


Fig.5 Wandering Particle Orbit in Region II for $e^2=4$, $s^2=0.040$, $\beta^2=0.25$,
 $q_+ = q_- = 0.5$

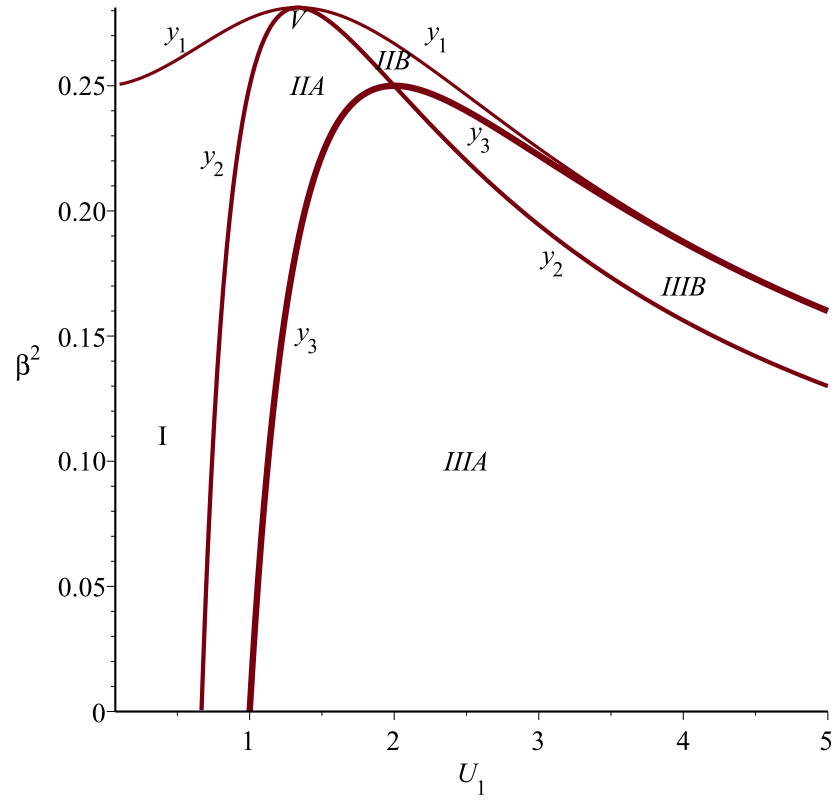


Fig.6 Boundaries for Regions I, II, and III for Light Trajectories

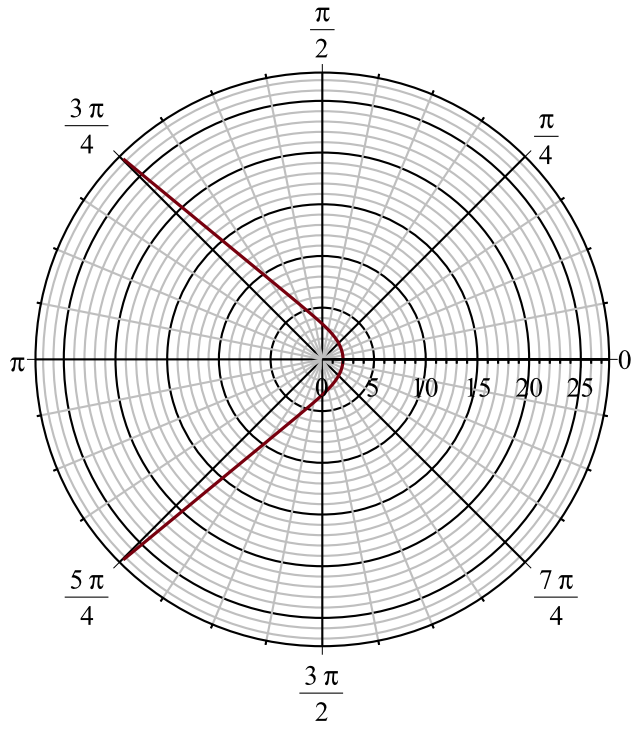


Fig.7 A Bent Light Trajectory in Region I for $U_1=0.42922$, $\beta^2=0.1$, $q_+=0.8873$, $q_-=0.1127$, $\Delta\varphi=81.4$ deg

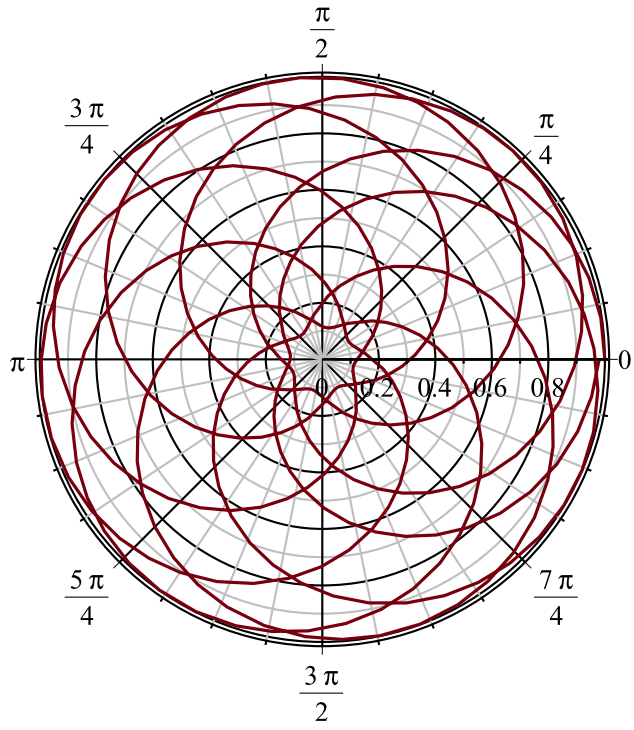


Fig.8 A Wandering Light Trajectory in Region II for $U_1=1$, $\beta^2=0.1$, $q_+=0.8873$, $q_-=0.1127$

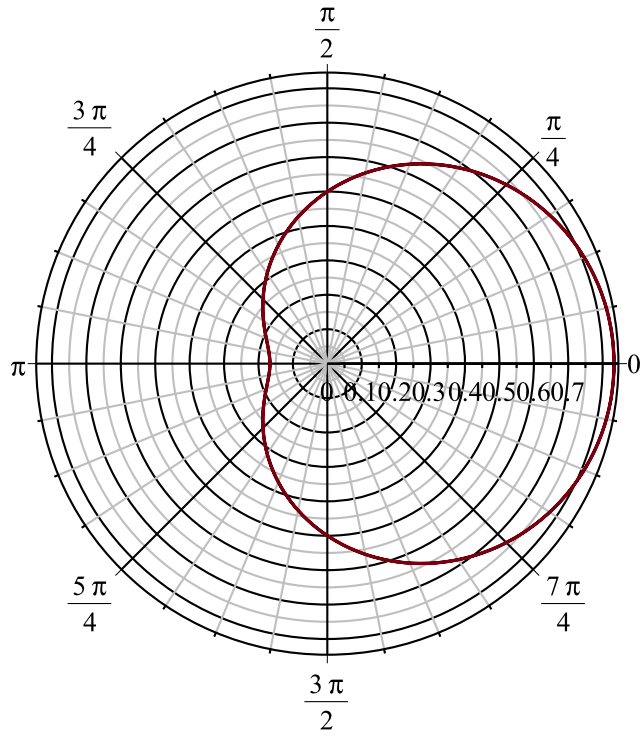


Fig.9 A Closed Light Trajectory on the Boundary of Regions II and III
for $U_1=1.2$, $\beta^2=0.13889$, $q_+=0.83333$, $q_-=0.16667$